Xyloglucan endotransglucosylase/hydrolase (XTH) overexpression affects growth and cell wall mechanics in etiolated *Arabidopsis* hypocotyls

Eva Miedes , Dmitry Suslov , Filip Vandenbussche , Kim Kenobi , Alexander Ivakov , Dominique Van Der Straeten, Ester P. Lorences , Ewa J. Mellerowicz , Jean-Pierre Verbelen and Kris Vissenberg

Abstract

Growth and biomechanics of etiolated hypocotyls from *Arabidopsis thaliana* lines overexpressing xyloglucan endotransglucosylase/hydrolase AtXTH18, AtXTH19, AtXTH20, and PttXET16-34 were studied. Overexpression of AtXTH18, AtXTH19, and AtXTH20 stimulated growth of hypocotyls, while PttXET16-34 overexpression did not show this effect. *In vitro* extension of frozen/thawed hypocotyls measured by a constant-load extensiometer started from a high-amplitude initial deformation followed by a slow time-dependent creep. Creep of growing XTH-overexpressing (OE) hypocotyls was more linear in time compared with the wild type at pH 5.0, reflecting their higher potential for long-term extension. XTH-OE plants deposited 65–84% more cell wall material per hypocotyl cross-sectional area than wild-type plants. As a result, their wall stress under each external load was lower than in the wild-type. Growing XTH-OE hypocotyls had higher values of initial deformation·stress^{-1} compared with the wild type. Plotting creep rates for each line under different loads against the respective wall stress values gave straight lines. Their slopes and intercepts with the abscissa correspond to φ (*in vitro* cell wall extensibility) and y (*in vitro* cell wall yield threshold) values characterizing cell wall material properties. The wall material in XTH-OE lines was more pliant than in the wild type due to lower y values. In contrast, the acid-induced wall extension *in vitro* resulted from increasing φ values. Thus, three factors contributed to the XTH-OE-stimulated growth in *Arabidopsis* hypocotyls: their more linear creep, higher values of initial deformation·stress^{-1}, and lower y values.

Key words: *Arabidopsis* hypocotyl, cell wall, creep test, extensiometry, growth, XTH

Introduction

The primary cell wall of flowering plants consists of cellulose fibrils tethered by hemicelluloses (principally xyloglucans) and embedded in an amorphous matrix of pectins and glycoproteins (Carpita and Gibeaut, 1993). Plant cell expansion is mainly regulated by cell wall extensibility (Cosgrove, 1993; Szymanski and Cosgrove, 2009) and results from selective loosening and rearrangement of the load-bearing cellulose/xyloglucan network, at least in flowering plants with Type I cell walls where xyloglucan is a predominant hemicellulose. Expansins are a class of proteins that are believed to break the load-bearing hydrogen bonds between xyloglucans and cellulose, thereby increasing cell wall extensibility (Cosgrove, 2000). Xyloglucan endotransglucosylase/hydrolases (XTHs), another class of cell wall-modifying proteins, also have the capacity to loosen cell walls (Nishitani and Vissenberg, 2007). Most XTHs cut and rejoin xyloglucan by xyloglucan endotransglucosylase (XET; EC 2.4.1.207) action, whereas some XTHs hydrolyse xyloglucan by xyloglucan hydrolase (XEH; EC 3.2.1.151) action (Rose *et al.*, 2002; Baumann *et al.*, 2007; Ibatullin *et al.*, 2009). Both activities may affect cell expansion. It was indeed found that XTH expression and XET activity correlate with growth (Vissenberg *et al.*, 2000, 2005), while alterations in XTH expression (Matsui *et al.*, 2005; Osato *et al.*, 2006) and exogenous addition of XET enzymes affect growth (Maris *et al.*, 2009). In order to check whether XTH regulates expansion, and, if so, whether this results from changes in cell wall mechanics, growth of hypocotyls of etiolated *Arabidopsis thaliana* (L.) Heynh. plants overexpressing different XTHs was studied and their *in vitro* extension was measured using constant-load extensiometry.

Until very recently, studies of different physical properties of *Arabidopsis* cell walls that could correlate with their *in vivo* extensibility were carried out using three techniques: breaking-force measurement (Reiter *et al.*, 1993), three-point bending test (Turner and Somerville, 1997), and the stress/strain method (Köhler and Spatz, 2002; Soga *et al.*, 2002; Ryden *et al.*, 2003). The bending test was performed with non-growing parts of *Arabidopsis* inflorescences, and the obtained values of wall strength and stiffness were not related to growth and cell wall extensibility (Turner and Somerville, 1997; Bichet *et al.*, 2001; MacMillan *et al.*, 2010). Breaking-force measurements were carried out with growing apical parts of inflorescences (Reiter *et al.*, 1993; Vanzin *et al.*, 2002). The value of breaking force has, however, no obvious correlation with the wall's ability to extend. Weaker cell walls are not necessarily more extensible than stronger ones, which is illustrated by *mur1* plants having a reduced breaking force of inflorescences and a dwarf phenotype (Reiter *et al.*, 1993). Stress/strain measurements in *Arabidopsis* were usually performed on etiolated hypocotyls. This organ elongates without accompanying cell divisions and serves as a model for studying the mechanism of expansion growth in plants (Gendreau *et al.*, 1997). Unfortunately, the stress/strain measurements were done either in basal parts of *Arabidopsis* hypocotyls (Ryden *et al.*, 2003; Peña *et al.*, 2004; Abasolo *et al.*, 2009), where cells had already ceased growing (Gendreau *et al.*, 1997), or in central segments of hypocotyls (Cavalier *et al.*, 2008) that have the lowest growth rate within this organ (Gendreau *et al.*, 1997). Thus, all these physical measurements with *Arabidopsis* cell walls have not been optimized for determining their properties relevant for growth. Information on such properties is greatly needed taking into account the ever-growing usage of *Arabidopsis* in plant research.

Among all *in vitro* tests for measuring cell wall physical properties, the creep (constant-load) method seems to give the best approximation of *in vivo* cell wall extensibility. Its advantage consists of the fact that a constant stress used during creep measurements mimics the action of turgor on growing cell walls better than a variable stress used in stress/strain (Taiz, 1984) and *in vitro* stress relaxation (Yamamoto, 1996) methods. Additionally, the constant-load method has a much higher resolution in revealing the time-dependent protein-mediated wall extension properties compared with other methods (Cosgrove, 1989). It is the creep method that allowed the discovery of expansins and yieldins, at that time new classes of cell wall proteins involved in growth regulation (McQueen-Mason *et al.*, 1992; Okamoto-Nakazato *et al.*, 2000). The constant-load method has started being used in *Arabidopsis* research very recently: first in connection with the control of gravitropism in hypocotyls (Vandenbussche *et al.*, 2011) then in petioles and hypocotyls in relation to the role of xyloglucans in primary cell walls (Park and Cosgrove, 2012*a*, *b*). The advantages of the creep method were used here to measure the wall physical properties of *Arabidopsis* hypocotyls relevant for growth and to demonstrate that the overexpression of *XTH* genes made the walls more extensible by a mechanism different from that of expansins. The *Arabidopsis* *AtXTH18*, *AtXTH19*, and *AtXTH20* genes overexpressed in the present study are closely related root-specific *XTH* genes that diversified by gene duplications. Despite their relatedness, they have very different expression patterns in root tissues, implying different roles for the respective XTHs in growth and development (Vissenberg *et al.*, 2005). The heterologous *XTH*, *PttXET16-34*, overexpressed here in *Arabidopsis*, encodes the enzyme involved in the growth of xylem cells in aspen (Nishikubo *et al.*, 2011). This XTH increased the diameter but not the length of vessel elements, thus affecting the cell growth anisotropy. By overexpressing these enzymes with potentially different functions, it was found that only *Arabidopsis* but not aspen XTHs affected growth of etiolated *Arabidopsis* hypocotyls.

Materials and methods

Plant material and growth conditions

Arabidopsis thaliana plants were grown *in vitro* in ES medium (Estelle and Somerville, 1987). The seeds were stratified for 3 d at 4 °C, exposed to light for 4 h, and the plants were grown in darkness at 20 °C for 7 d. To distinguish growth-relevant mechanical properties from those having no relationship to growth, 5 mm long segments of hypocotyls starting from 1.5 mm below the cotyledons were investigated in 4- and 7-day-old etiolated plants (Supplementary Fig. S1 available at *JXB* online). These subapical segments contain the main part of the growth zone in 4-day-old seedlings (Supplementary Fig. S1A) and comprise essentially no

expanding cells in 7-day-old seedlings (Supplementary Fig. S1B). The segments were extended in biomechanical tests and used in all biochemical and molecular analyses reported here, with the exception of *in vivo* growth measurements.

Generation of XTH-overexpressing lines

To shed light on the role of XTH in the regulation of growth and biomechanics, four *Arabidopsis* transgenic lines overexpressing *AtXTH18*, *AtXTH19*, *AtXTH20*, and *PttXET16-34* were generated in the Col-0 background. The *Arabidopsis* XTH-overexpressing (OE) constructs were made by isolating the full-length coding sequence of *AtXTH18*, *AtXTH19*, and *AtXTH20* from *Arabidopsis* seedling cDNA by PCR using AttB1 and AttB2 primer sets, followed by subcloning into pDONR207 (Invitrogen) according to the manufacturer's instructions. The sequence-verified PCR fragments were then introduced into pH2GW7.0 (Karimi *et al.*, 2002) (LR reaction) for *Cauliflower mosaic virus* 35S-driven expression. The coding region of *PttXET16-34* (*AF515607*), clone A033P02U (http://www.populus.db.umu.se/), was cloned in the sense orientation into the *Bam*HI restriction site of the pPCV-702kana binary vector (Walden *et al.*, 1990) behind the *35S* promoter. All primer sequences are listed in Supplementary Table S1 at *JXB* online.

Plants were transformed using the flower dip method (Clough and Bent, 1998). Standard lines were established by isolating T_3 plants homozygous for the transgene. Twelve, nineteen, ten, and four independent transgenic plants were generated for *AtXTH18*, *AtXTH19*, *AtXTH20*, and *PttXET16-34* expression constructs, respectively. Then one transgenic line for each construct was selected showing the maximal level of overexpression as determined by real-time semi-quantitative reverse transcription–PCR (semi-qRT–PCR) on leaves (for details, below).

Analysis of XTH expression levels using real-time qRT-PCR

To analyse the actual levels of *XTH* overexpression in the tissue of interest, the 5 mm long subapical segments of etiolated hypocotyls (~100 mg) were collected and total mRNA was extracted with TRIzol® Reagent according to the manufacturer's instructions (Invitrogen). RNA was quantified by absorbance at 260 nm. After the treatment with RNase-free DNase (Promega), total mRNA was reverse transcribed using the First-Strand cDNA Synthesis SuperScript™ II Reverse Transcriptase (Invitrogen) with RNase OUT (Recombinant Ribonuclease Inhibitor, Invitrogen).

The PCR amplification was performed with gene-specific primers. Primer sequences for the *AtXTH18*, *AtXTH19*, *AtXTH20*, and *PttXET16-34* genes, and elfα-1 and 18S, the housekeeping genes used as internal controls, are listed in Supplementary Table S1 at *JXB* online.

The first screenings were performed by real-time semi-qRT–PCR. PCR conditions for 31 cycles were as follows: 5 s at 95 °C, 60 s at 60 °C, and 30 s at 72 °C. The overexpression was evaluated by analysis of gel images.

Selected lines were analysed by real-time qRT–PCR. Two replicates were performed for each sample in a final volume of 25 µl containing 1 µl of cDNA, 25 pmol XTH- or internal control-specific primers, and 12.5 µl of Maxima™s SYBR Green qPCR Master Mix (Fermentas) according to the manufacturer's instructions. PCRs were carried out using the LightCycler (Roche) for 10 min at 95 °C (initial denaturation) and then for 40 cycles as follows: 15 s at 95 °C, 60 s at 60 °C, and 30 s at 72 °C. Each real-time curve was tested using a dissociation protocol to ensure that each amplicon was a single product. The efficiency of the primers was evaluated according to Roche's instructions, and the relative expression ratio of the target genes was based on primer efficiency and Ct values, and this was normalized to both internal controls (Pfaffl, 2001), giving identical results.

Growth analysis

To study the effect of *XTH* overexpression on growth of hypocotyls, XTH-OE lines and wild-type Col-0 seeds were grown on ES medium and treated as mentioned above. Etiolated growth was measured with an infrared imaging system that records pictures regularly at fixed time intervals as described in Vandenbussche *et al.* (2010). Plates with seeds were placed vertically to allow growth in a plane parallel with the detector of the cameras. The length of the hypocotyls was evaluated every 24 h using ImageJ software (public domain: http://rsb.info.nih.gov/ij/).

XET and XEH activities

In order to establish whether *XTH* overexpression affects total XET and XEH activities, soluble and ionically bound proteins were extracted by homogenization of partially thawed 5 mm long subapical segments of *Arabidopsis* hypocotyls in 200 mM sodium acetate pH 5.8 as previously described (Miedes and Lorences, 2004). The protein content of the extracts was assessed according to Bradford (1976).

XET activity was assayed as previously described (Fry *et al.*, 1992; Miedes and Lorences, 2009). Reaction mixtures (total volume 40 µl) containing 5 mg ml^{-1} of partially purified tamarind xyloglucan, 0.85 kBq of [^{3}H]XXXGol (prepared as described in Lorences and Fry, 1993), sodium acetate 50 mM pH 5.8, and 25 µl of extract (0.5–0.6 mg ml^{-1}) were incubated for 1 h at 25 °C. The reaction was stopped by the addition of 100 µl of 20% (w/v) formic acid, and the solution was then dried on 5 × 5 cm Whatman 3MM filter paper, washed for 30 min in running tap water to remove free [^{3}H]XXXGol, re-dried, and assayed for ^{3}H by scintillation counting (Wallac 1410, Pharmacia, Canada). Inactivated controls were carried out in the same way using heat-inactivated enzymes (boiled for 30 min).

XEH activity was assayed by viscosity and reducing sugar assays. The reaction mixtures contained 500 µl of 1% tamarind xyloglucan (Megazyme) in 50 mM sodium acetate pH 5.8 and 250 µl of the same buffer supplemented with 50 µg of protein or 50, 10, 5, and 2.5 µg of cellulase from *Trichoderma viride* (Onozuka R-10, Serva) which was used as a positive control. The viscosity of the mixtures was estimated after 0, 15, 30, and 60 min, and 12 h of incubation at room temperature (20 °C) as a function of their flow rate through 200 µl pipettes. The flow time was determined three times for each sample and the relative viscosity was calculated. The reducing sugar assay was performed for the same samples by the Nelson–Somogyi method (Nelson, 1944; Somogyi, 1952).

FT-IR analysis

To study whether *XTH* overexpression influences the cell wall composition, Fourier transform infrared spectroscopy (FT-IR) was performed as described in Miedes *et al.* (2011) using 5 mm long subapical segments of *Arabidopsis* hypocotyls. A total of 128 interferograms were collected for each sample in transmission mode at 8 cm^{-1} resolution using a Thermo-Electron instrument. All spectra were baseline-corrected and area-normalized (800–1800 cm^{-1}) using Omnic software. Principal component analysis (PCA) and *t*-tests were performed with Statistica 9.1 software using a maximum of five principal components.

Extensiometry

To establish whether overexpression of *XTH* genes changes the biomechanics of hypocotyls, the constant-load (creep) method was used. Etiolated *Arabidopsis* seedlings were transferred individually into Eppendorf test tubes, frozen by plunging the closed tubes into liquid nitrogen, stored at −20 °C, and used for extensiometry within 2 weeks after freezing.

In vitro extension of frozen/thawed *Arabidopsis* hypocotyls was measured with a custom-built constant-load extensiometer described in Suslov and Verbelen (2006) using the same procedure as in

Vandenbussche *et al.* (2011). A 5 mm long hypocotyl segment (starting from 1.5 mm below the cotyledons) was secured in the extensiometer and pre-incubated in a buffer (20 mM MES-KOH, pH 6.0 or 20 mM Na-acetate, pH 5.0) in the relaxed state for 2 min, after which it was extended in the same buffer under a constant load. *Arabidopsis* hypocotyls taper significantly and, accordingly, become very weak close to the apical hook. Due to this weakness, a part of the growth zone located next to the cotyledons was not analysed in extensiometry (Supplementary Fig. S1A at *JXB* online). The exact values of the *in vivo* wall stress are unknown for *Arabidopsis* hypocotyls. So, the three constant loads used here (500, 625, and 750 mg) were chosen for inducing the broadest possible range of creep rates: from minimal, close to the limit of detection (500 mg), to maximal (750 mg), approaching the threshold after which hypocotyls break.

For all the variants studied, 1–3 recordings of *in vitro* hypocotyl extension were made for 60 min to characterize the shape of long-term creep curves, while the majority of recordings were made for 15 min only (Supplementary Fig. S2 at *JXB* online). The creep kinetics were similar when comparing 5–15 min versus 15–60 min segments of extension curves (Supplementary Fig. S2). Thus, the data obtained from the analysis of 15 min long recordings can be extrapolated to a long-term creep. The *in vitro* extension was measured during the intervals 0 s to 5 s (initial deformation, I), 5 s to 5 min (creep amplitude 5 s–5 min, C_5), 5 min to 10 min (creep amplitude 5 min–10 min, C_{10}), and 10 min to 15 min (creep amplitude 10 min–15 min, C_{15}) after loading. The average creep rate was calculated during the interval 5–15 min after loading in % h^{-1} using the formula $(\ln L_{15min} - \ln L_{5min})/T \times 100\%$ adapted from Green (1976) and Thompson (2008). Here L_{15min} and L_{5min} indicate the length of an extending hypocotyl segment at 15 min and 5 min after loading, respectively. T is the time during which the average creep rate is calculated (10 min). L_{5min}=5 mm (length of the hypocotyl segment before stretching)+I+C_5. Accordingly, L_{15min}=5 mm+I+C_5+C_{10}+C_{15}. The linearity of creep of hypocotyl segments was estimated as C_{15}/C_{10}. Initial deformation refers to a practically instantaneous, high-amplitude strain taking place just after loading. In practice it was measured 5 s after a load application to eliminate mechanical artefacts: loading usually causes a short-term (<5 s) vibration of the sensor's core recorded in extension curves as high frequency oscillations.

Determination of cross-sectional area and tensile stress in hypocotyl segments

In vitro extension of hypocotyls in the creep test is proportional to the stress (a force divided by the cross-sectional area across which it acts) developing in their cell walls under the action of a constant load. To calculate this stress, the cross-sectional area of the hypocotyl cell walls was determined using a classical method of Cleland (1967) based on measuring the wall dry weight per hypocotyl unit length. It is assumed that the wall density (ρ) is 1.5 g cm^{-3} (Gibson, 2012). By definition, $\rho = m/V$, where m is mass and V is volume. For a segment of a cylindrical organ such as hypocotyl, $V = l \times A$, where l is length of the segment (5 mm) and A is its cross-sectional area. From the above equations, $A = m/(\rho \times l)$ and can easily be calculated using the known length of hypocotyls segments (5 mm) and their measured mass, and assuming that ρ=1.5 g cm^{-3}.

Cell walls from 5 mm long segments of *Arabidopsis* hypocotyls were dehydrated according to Miedes *et al.* (2011). The weight of the dry wall material prepared from 50 segments (5 mm long) of *Arabidopsis* hypocotyls was determined using a Mettler M3 balance with a resolution of 1 µg.

The tensile stress (MPa) developing during the uniaxial extension of *Arabidopsis* hypocotyls *in vitro* under a constant load was calculated as the ratio F/A [F, tensile force (N); A, hypocotyl cross-sectional area (m^2)]. The loads 500, 625, and 750 mg used in extensiometry generated tensile forces of 0.00490, 0.00613, and 0.00735 N, respectively.

Analysis of statistical data

If not stated otherwise, all statistical analyses were carried out with IBM SPSS Statistics 19.0. Comparisons between two groups (differences between 4- and 7-day-old hypocotyls as well as between treatments at pH 6 and pH 5) were performed using a Student's two-tailed t-test. If not stated otherwise, multiple comparisons between the wild type and the four XTH-OE lines involved analysis of variance (ANOVA) followed by Dunnett's (homogenous variances and equal number of repeats in the groups to be compared) or Games–Howell's (non-homogenous variances and/or unequal number of repeats in the groups to be compared) post-hoc tests. The homogeneity of variances was analysed using Levene's test.

The dependence of creep rate on the wall stress was estimated by fitting Model II linear regression models with errors in both variables using the Maximum Likelihood Functional Relationship implementation from Ripley and Thompson (1987), a variant of Deming regression, assuming the residual standard error is proportional to the standard error of the sample. The code of the method is available at https://stat.ethz.ch/pipermail/r-help/2010-February/227865.html. *In vitro* cell wall extensibility was estimated as the slope of the regression line, with stress as the independent variable and creep rate as the dependent variable. The *in vitro* yield threshold was estimated by regressing stress as a dependent variable on creep rate as the independent variable and taking the intercept of this line. This is a valid approach because the Maximum Likelihood Functional Relationship method is symmetric and gives the same result, regardless of whether x is regressed on y or y on x, as pointed out in Ripley and Thompson (1987). Standard errors for the slope and intercept were derived using leave-one-out jackknife. Non-parametric estimates of the means and variances of the ratios creep rate·$stress^{-1}$ and initial deformation·$stress^{-1}$ were obtained using random bootstrap resampling with 10 000 iterations. Comparisons of the ratio estimates between groups were then performed using a Student's two-tailed t-test with 14 degrees of freedom and corrected for multiple comparisons by maintaining the false discovery rate at 5% (Benjamini and Hochberg, 1995).

Accession numbers

Sequence data from this article can be found at The Arabidopsis Information Resource (TAIR, www.Arabidopsis.org) under the following accession numbers (*AtXTH18*, At4g30280; *AtXTH19*, At4g30290; *AtXTH20*, At5g48070; and *PttXET16-34*, AF515607).

Results

Arabidopsis *plants overexpressing XTHs*

Arabidopsis plants stably overexpressing *AtXTH18*, *AtXTH19*, *AtXTH20*, and an aspen *XTH* (*PttXET16-34*) were generated. For each of the above *XTH* genes, one line showing the highest overexpression was selected using semi-qRT–PCR on leaves. The *XTH* overexpression in 5 mm long subapical segments of dark-grown hypocotyls was quantified using real-time qRT–PCR. The relative expression level of *AtXTH18*, *AtXTH19*, and *AtXTH20* was two, seven, and 29 times higher in 4-day-old hypocotyls of the overexpression lines compared with the wild type, and one, 60 and 72 times higher in 7-day-old hypocotyls, respectively.

Growth kinetics of etiolated hypocotyls

In order to establish whether *XTH* overexpression affects growth, changes in length of etiolated hypocotyls were monitored during the whole period of their elongation. It was found that growth ceased after 5 d in the AtXTH18-OE line and after 7 d in the rest of the studied lines (Fig. 1A, B).

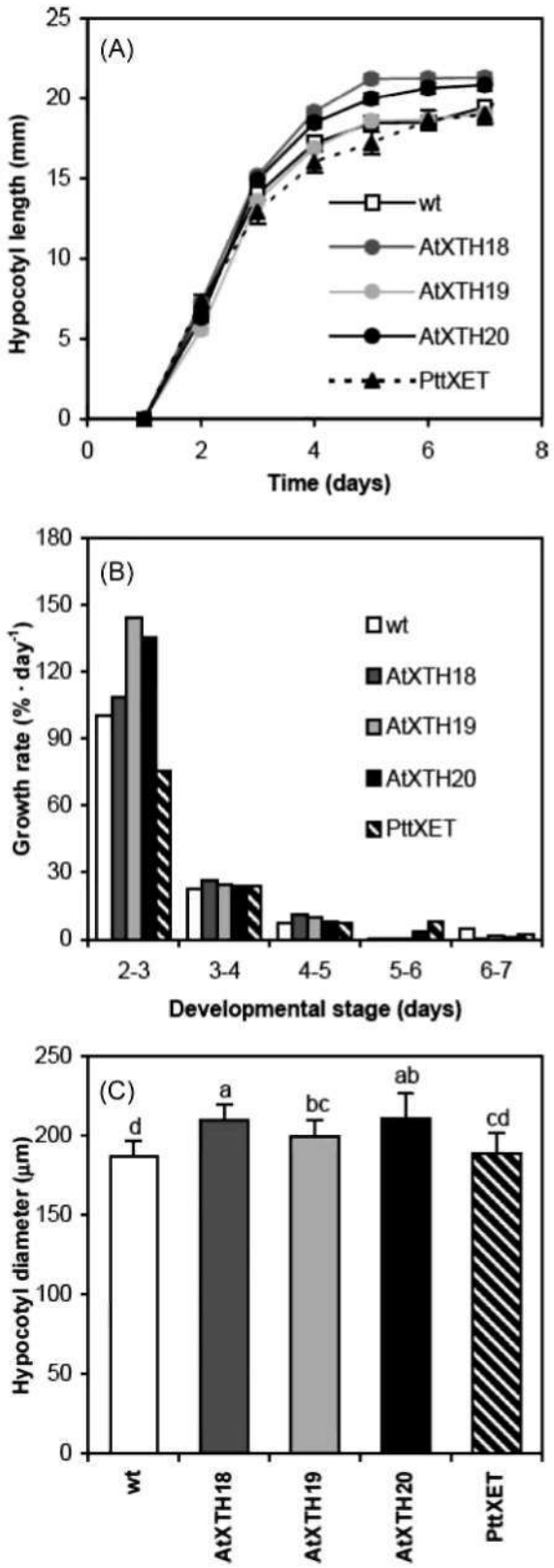

Fig. 1. *In vivo* elongation kinetics and diameter measurements of dark-grown *Arabidopsis* hypocotyls overexpressing different XTHs versus the wild type. (A) Growth of different XTH-OE lines versus the wild type. Data are means ±SE (n=31–65). For the majority of the lines studied, error bars are smaller than symbols. (B) Average growth rate of hypocotyls in 2- to 7-day-old etiolated *Arabidopsis* plants. The rate is calculated for each 1 d-long period during hypocotyl development from the data of Supplementary Table S2 at *JXB* online. (C) Measurements of the diameter of 4-day-old *Arabidopsis* hypocotyls. Data are means ±SD (n=19–40). *Arabidopsis* lines with significantly different hypocotyl diameters ($P < 0.05$, Games–Howell's post-hoc test performed after ANOVA) do not have identical letters above the respective bars on the plot.

Overexpression of *AtXTH18* and *AtXTH20* demonstrated the most prominent stimulatory effect on growth, and etiolated hypocotyls of AtXTH18- and AtXTH20-OE lines were significantly longer compared with the wild type from the age of 3 d and 4 d, respectively (Fig. 1A; Supplementary Table S2 at *JXB* online). The PttXET16-34-OE line displayed a similar growth pattern to the wild type with no significant differences in hypocotyl length (Supplementary Table S2). The AtXTH19-OE line demonstrated a more complex growth pattern compared with the different OE lines. Its hypocotyls were significantly shorter than wild-type hypocotyls in 2-day-old plants due to delayed germination and/or lower growth rate (Supplementary Table S2). On subsequent days, however, they reached the length of wild-type hypocotyls because of faster elongation (Fig. 1B). Thus, all lines overexpressing the *Arabidopsis XTH* genes showed higher hypocotyl elongation rates during at least a part of their growth cycle. In addition, hypocotyls of AtXTH18-, AtXTH19-, and AtXTH20-OE lines, in contrast to those of the PttXET16-34-OE line, were significantly thicker than wild-type hypocotyls (Fig. 1C). It was concluded that only the *Arabidopsis* XTHs but not the aspen XTH stimulate growth in both length and diameter, when overexpressed in etiolated *Arabidopsis* hypocotyls.

Xyloglucan endotransglucosylase (XET) and xyloglucan endohydrolase (XEH) activities

The effect of *XTH* overexpression on xyloglucosyltransferase (EC 2.4.1.207) and hydrolase (EC 3.2.1.151) activities was analysed in the 5 mm long subapical segments of etiolated 4- and 7-day-old *Arabidopsis* hypocotyls. The enzymic activity measured reflected the contribution of all, not only the overexpressed, XTH proteins present in the tissue.

XET activity determined using a radiometric technique doubled between day 4 and day 7, indicating an accumulation of XTHs in cell walls (Fig. 2A). Only the PttXET16-34-OE line showed significantly higher XET activity compared with the wild type at both ages.

XEH activity was evaluated by two different methods. The first method quantified reducing sugars produced by hydrolase activity on xyloglucan. After 1 h incubation of the hypocotyl protein samples with the substrate (Fig. 2B), or even after 12 h of incubation (data not shown), the amount of reducing sugars was barely detectable in 4- and 7-day-old hypocotyls, whereas the positive control showed clear activity. In the viscosimetric method, the ability of the enzyme to hydrolyse xyloglucan, thereby reducing its viscosity, was studied. None of the lines showed detectable XEH activity at the three time points up

to 60 min of incubation (Fig. 2C, D) or even after prolonged incubation for 12 h (data not shown), consistent with results for *in vitro* enzymic activity of AtXTH18, AtXTH19, AtXTH20 (Maris *et al.*, 2011), and PttXET16-34 (Kallas *et al.*, 2005). In the positive control xyloglucan was clearly hydrolysed by cellulase, even at low enzyme concentrations.

Estimation of cell wall composition by FT-IR

In order to reveal qualitative differences in cell wall composition of *Arabidopsis* hypocotyls, FT-IR analysis was performed. Student's *t*-test on comparison between average spectra from the XTH-OE lines against the wild type showed few significant differences (Supplementary Fig. S3, Supplementary Table S3 at *JXB* online). In 4-day-old growing hypocotyls they were limited to an increase in phenols and protein with a concomitant decrease in polygalacturonic acid and galactose in the PttXET16-34-OE line compared with the wild type. These changes may be linked with the fact that it was the only XTH-OE line showing no growth effect (Fig. 1A, B; Supplementary Table S2). The relatively similar wall composition of the wild type and XTH-OE lines at the same age was in a sharp contrast to numerous significant differences between 4- and 7-day-old hypocotyl walls of the respective lines (compare *t*-values in Supplementary Figs S3 and S4, and in Supplementary Tables S3 and S4). This finding was also confirmed by PCA that clearly distinguished two groups according to the age of the hypocotyls (Supplementary Fig. S5). The most prominent age-dependent changes involved pectin de-esterification along with the accumulation of mannans

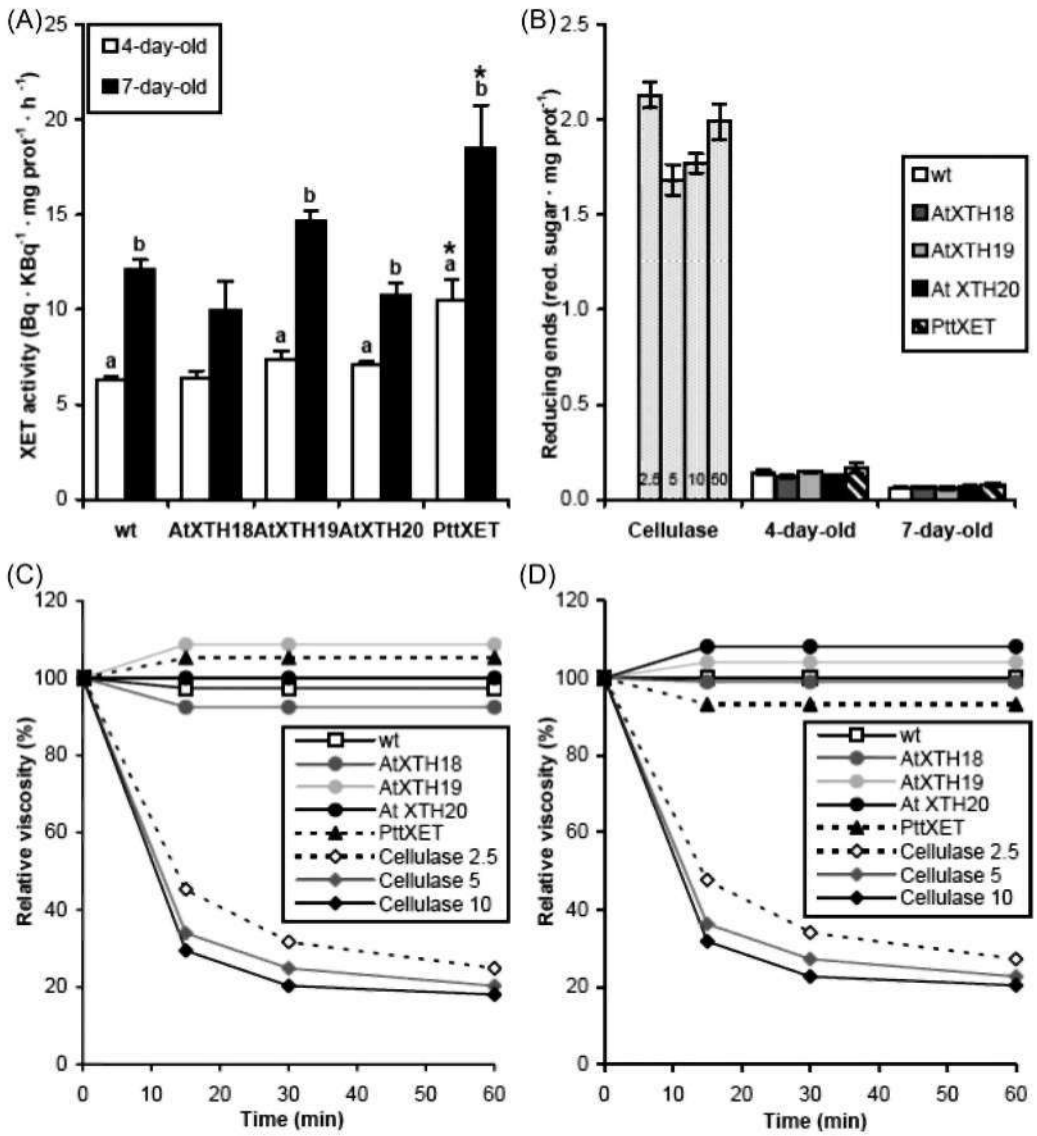

Fig. 2. XET and XEH activities of XTH-overexpressing lines. (A) XET activity measured by the radiometric method. Data are means ±SE (n=3). Different lower case letters mark significant differences ($P < 0.05$, Student's two-tailed t-test) in XET activity between 4- and 7-day-old hypocotyls of the same *Arabidopsis* line. Asterisks mark significant differences ($P < 0.05$, Dunnett's post-hoc test performed after ANOVA) in XET activity of XTH-OE lines versus the wild type when comparing hypocotyls of the same age. (B) XEH activity determination using the colorimetric assay after 1 h incubation of protein samples from the

and cellulose (Supplementary Table S4). Pectin de-esterification can contribute to the developmental growth cessation in hypocotyls (Fig. 1A) via calcium-mediated cross-linking (Jarvis, 1984). Accumulation of mannans and cellulose may reflect secondary cell wall deposition in the course of vascular differentiation in maturing hypocotyls (Handford *et al.*, 2003).

Estimation of cell wall mechanical properties

XTH overexpression induced an increase in hypocotyl diameter (Fig. 1C). This may have profound consequences for biomechanics if a concomitant increase in the wall cross-sectional area takes place. Cell wall extension is proportional to the stress (= force divided by the cross-sectional area across which it acts) resulting from a constant load (*in vitro*) or turgor (*in vivo*). Thus, depending on the wall cross-sectional area, the same load can generate different stresses inducing different hypocotyl extension. So cell wall cross-sectional areas were determined by measuring the wall dry weight per hypocotyl unit length (Cleland, 1967). In 4-day-old hypocotyls of all the XTH-OE lines, the cross-sectional areas were significantly higher (by 65–84%) than in the wild type, while in 7-day-old hypocotyls this difference was smaller (Supplementary Table S5). Therefore, each constant load generates a proportionally higher stress in wild-type cell walls (Supplementary Table S5), especially in growing 4-day-old hypocotyls.

In vitro extension of frozen/thawed *Arabidopsis* hypocotyls in a creep test started from a practically instantaneous high-amplitude strain (initial deformation) followed by a slow time-dependent deformation (creep) (Supplementary Tables S6–S8 at *JXB* online). Initial deformation and creep were considered separately, because they may reflect different wall properties with a different relationship to plant growth.

Initial deformations did not differ significantly between wild-type and XTH-OE hypocotyls under the same load (Supplementary Tables S6–S8 at *JXB* online). Replacing the loads by the respective wall stress values (Supplementary Table S5) revealed that equivalent initial deformations were achieved in growing hypocotyls of XTH-OE lines at much lower wall stress than in the wild type (Supplementary Fig. S6A, C). To assess the influence of these differences in wall stress statistically, the ratios initial deformation·stress^{-1} were determined and found to be significantly higher in 4-day-old hypocotyls of all the XTH-OE lines versus the wild type (Fig. 3A, C). The increased normalized initial deformations in the XTH-OE lines (Fig. 3) could be a factor contributing to their higher growth (Fig. 1). Initial deformations were not stimulated under acidic conditions, being numerically lower at pH 5.0 than at pH 6.0. In several cases, these differences were statistically significant (Fig. 3; Supplementary Tables S6–S8). Additionally, initial deformations decreased in 7-day-old non-growing versus 4-day-old growing hypocotyls (Fig. 3; Supplementary Tables S6–S8).

A preliminary study of *Arabidopsis* hypocotyl creep curves has shown that their shape may differ depending on the line and treatment (Supplementary Fig. S2 at *JXB* online). To better illustrate the dependence of the creep curve shape on age, genotype, and pH, average curves of *in vitro* extension under a constant load were generated (Fig. 4). It was found that the average creep curves of 4-day-old hypocotyls in all XTH-OE lines under a 625 mg load were more linear at pH 5.0 than at pH 6.0 (Fig. 4A, C). Moreover, 7-day-old hypocotyls obviously lost their capacity for linear extension at pH 5.0 in comparison with 4-day-old hypocotyls (Fig. 4C, D). To assess statistical differences in the shape of extension curves, a simple index of curvature was developed. For each curve, its creep amplitude between 10 min and 15 min was divided by that between 5 min and 10 min (Supplementary Fig. S2). The resulting index, referred to as 'linearity', showed how close the given experimental curve was to a straight line. The closer this index to unity, the more linear the extension curve. The calculated linearities (Supplementary Table S9) confirmed the observations from Fig. 4 and added some interesting details. Indeed, the linearity of extension in 4-day-old hypocotyls at pH 5.0 was usually higher than at pH 6.0, especially in AtXTH18-OE and AtXTH20-OE lines. The significant differences between different *Arabidopsis* lines were found only in growing 4-day-old hypocotyls at pH 5.0 where the extension of certain XTH-OE lines was more linear than in the wild type (Supplementary Table S9). This finding may suggest that XTH overexpression increases the wall capacity for a long-term extension. As for the age-dependent changes, the strong decrease in linearity of creep in 7-day-old versus 4-day-old hypocotyls at pH 5.0 was confirmed (compare Fig. 4C, D and Supplementary Table S9).

Taking into account differences in the wall stress under any given constant load, creep rates of *Arabidopsis* hypocotyls were compared (Supplementary Fig. S7 at *JXB* online). They were found to be highly pH dependent, being 3- to 5-fold higher at pH 5.0 compared with pH 6.0. Nevertheless, the relative differences in creep rate between the wild type and XTH-OE lines were rather similar in 4-day-old hypocotyls under all loads and at both pH values tested. Namely, the creep rate of wild-type hypocotyls was usually higher than that of XTH-OE lines (Supplementary Fig. S7A, C). This difference was greater at pH 5.0 than at pH 6.0. The lines overexpressing *AtXTH18* and *AtXTH20* were the least extensible in 4-day-old hypocotyls (Supplementary Fig. S7A, C). Surprisingly, there were no dramatic differences between the creep rates of growing 4-day-old and non-growing 7-day-old hypocotyls of the respective lines (Supplementary Fig. S7). In a few cases where significant age-related changes were observed, they were opposite for the different lines, with the wild type, AtXTH19-OE, and PttXET-OE demonstrating lower and AtXTH18-OE and AtXTH20-OE demonstrating higher creep rates in the more mature hypocotyls (Supplementary Fig. S7).

hypocotyls. Data are means ±SE (n=3). (C, D) XEH activity assay by the viscosimetric method using protein samples from (C) 4-day-old and (D) 7-day-old hypocotyls. Cellulase was used as a positive control. Cellulase 2.5, 5, 10, and 50 contained 2.5, 5, 10, and 50 µg of protein in the assay, respectively. Cellulase 50 was not included in (C) and (D) because the curve provided no additional information.

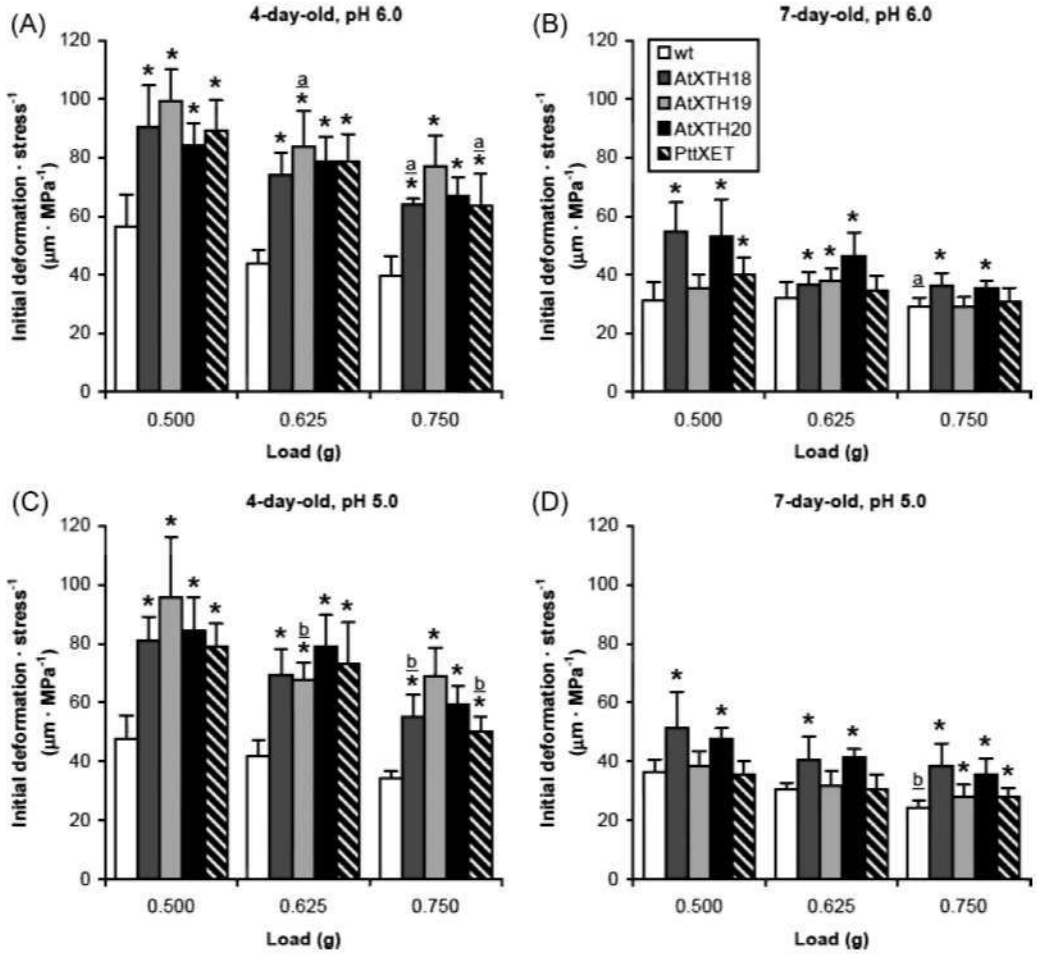

Fig. 3. Normalized initial deformations (initial deformation·stress $^{-1}$) of frozen/thawed *Arabidopsis* hypocotyls *in vitro*. These were calculated from the values of initial deformations and wall stress reported in Supplementary Tables S6–S8, and S5 at *JXB* online, respectively, and refer to (A) hypocotyls of 4-day-old plants extended at pH 6.0; (B) hypocotyls of 7-day-old plants extended at pH 6.0; (C) hypocotyls of 4-day-old plants extended at pH 5.0; (D) hypocotyls of 7-day-old plants extended at pH 5.0. Data are means ±SD obtained using random bootstrap re-sampling with 10 000 iterations. Asterisks mark significant differences ($P < 0.05$, Student's two-tailed *t*-test) in normalized initial deformations of XTH-OE lines versus the wild type within a group of hypocotyls of the same age extended under the same load and pH value. Different underlined letters on the bar charts mark significant differences ($P < 0.05$, Student's two-tailed *t*-test) in normalized initial deformation determined at pH 6.0 and pH 5.0 for hypocotyls of the same line and age extended under the same load. Normalized initial deformations for 7-day-old hypocotyls were always significantly lower than in 4-day-old hypocotyls ($P < 0.001$, Student's two-tailed *t*-test) for the respective variants (not shown on the plots).

Contraintuitively, creep rates of wild-type, AtXTH18- and AtXTH20-OE, hypocotyls (Supplementary Fig. S7 at *JXB* online) were inversely related to their *in vivo* growth rates (Fig. 1A, B). This relationship may be explained by the higher wall stress generated in the wild type than in the XTH-OE lines under each constant load (Supplementary Table S5). To compare differences in the wall material properties under identical stress conditions, the creep rates for different variants (Supplementary Fig. S7) were plotted against the calculated values of wall stress (Supplementary Table S5). The dependence of creep rate on wall stress was found to be linear (R^2 values from 0.93 to 0.99). The respective straight lines were fitted to the data (Fig. 5) using the Deming linear regression method taking into account the error in both creep rate (Supplementary Fig. S7) and wall stress (Supplementary Table S5), as well as the greatly different variances for creep rate and wall stress values. According to Okamoto and Okamoto (1994) the slopes of these lines correspond to φ values (*in vitro* cell wall extensibility), while their intercepts with the abscissa correspond to y values (*in vitro* cell wall yield threshold). The y value shows the minimal wall stress at which creep starts, and the φ value characterizes the sensitivity of creep rate to changes in wall stress. The φ and y values for the walls of the different *Arabidopsis* lines are given in Table 1. The acid-induced stimulation of creep in *Arabidopsis* hypocotyls was found to be achieved by raising φ. On the other hand, φ values did not demonstrate consistent changes as a result of the overexpression of XTHs. However, walls of 4-day-old hypocotyls of all XTH-OE lines had much lower y values (more optimal for high creep rate) than wild-type walls (Fig. 5A, C; Table 1). As regards 7-day-old hypocotyls of XTH-OE lines,

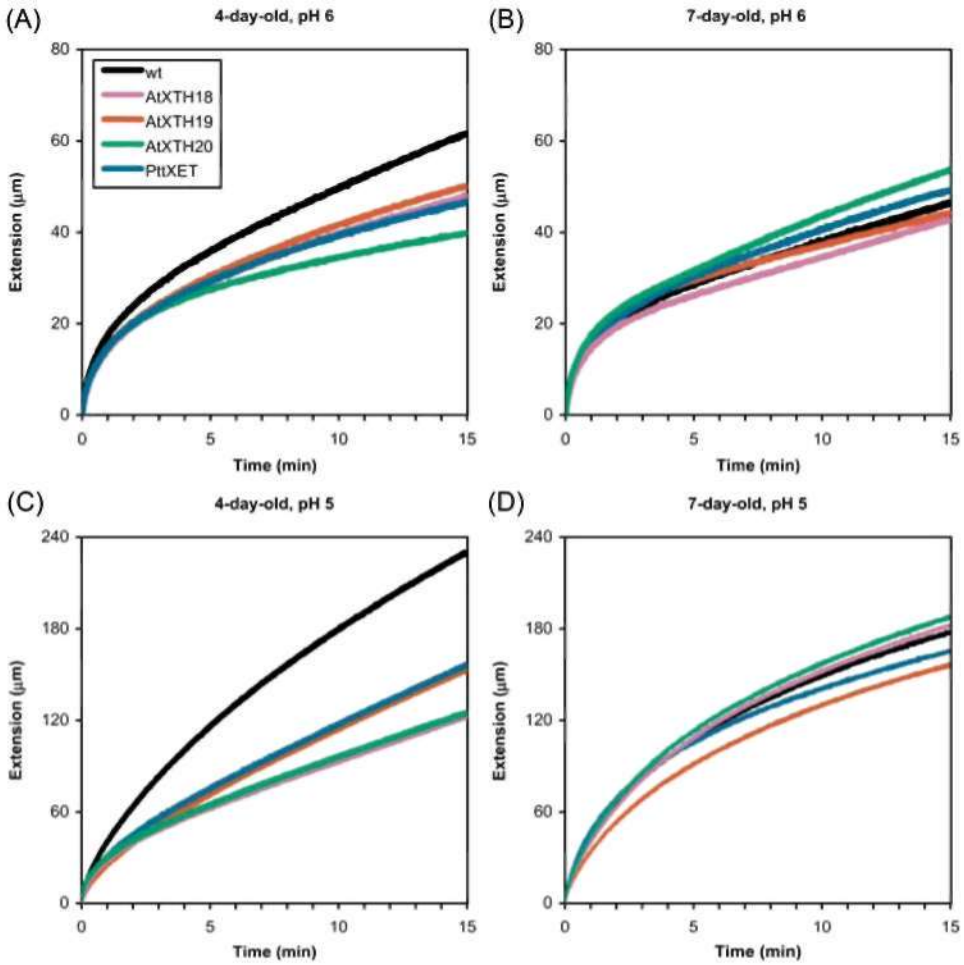

Fig. 4. Differences in shape of *in vitro* extension curves of frozen/thawed *Arabidopsis* hypocotyls. The reported curves were obtained using (A) hypocotyls of 4-day-old plants extended at pH 6.0; (B) hypocotyls of 7-day-old plants extended at pH 6.0; (C) hypocotyls of 4-day-old plants extended at pH 5.0; (D) hypocotyls of 7-day-old plants extended at pH 5.0. Each curve is the average of 8–10 experimental curves of hypocotyl extension under a 625 mg load. Before averaging, all experimental curves were baseline corrected by subtracting the respective initial deformation values. Note that the ordinate axes are scaled differently for the pH 6.0 (A, B) and the pH 5.0 (C, D) data.

their y values approached those of the wild type (Fig. 5B, D; Table 1). The age effects manifested themselves mostly in increasing y values in 7-day old versus 4-day old hypocotyls in all lines, with the exception of the wild type, while φ values did not demonstrate consistent changes (Table 1).

By analogy with initial deformations, creep rates were divided by their respective values of wall stress (Supplementary Fig. S8 at *JXB* online). The resulting normalized creep rates of 4-day-old hypocotyls were not consistently different between XTH-OE lines and the wild type (Supplementary Fig. S8A, C). In contrast to normalized initial deformations (Fig. 3A, C), normalized creep rates alone cannot explain why XTH-OE hypocotyls grow more quickly than wild-type controls (Fig. 1A, B). As XTH overexpression concomitantly decreases the y value of the wall material (Fig. 5) and increases its amount (Supplementary Table S5), the resulting growth rate will be dependent on the balance between these two effects: the first will apparently be stimulatory for cell expansion, while the second might be inhibitory.

To understand which cell wall biomechanical characteristics could contribute to the growth stimulation in the XTH-OE lines, a correlation analysis was performed (Supplementary Table S10 at *JXB* online). A moderate positive correlation was observed between the values of initial deformation·stress $^{-1}$ and growth rate under all tested conditions. No correlation was found between growth and φ values in the *Arabidopsis* lines studied. *In vitro* cell wall yield threshold demonstrated a moderate negative correlation with growth rate, suggesting that lower y values observed in the XTH-OE lines (Table 1) might have contributed to their higher growth rate (Fig. 1B). A strong positive correlation (R^2=0.80–0.89) was observed between linearity of creep at pH 5.0 under 625 mg and 750 mg loads and growth (Supplementary Table S10). Interestingly, creep rates under these conditions (5.3–16.3 % h^{-1}, Supplementary Fig. S7C) were very similar to *in vivo* cell growth rates (~7.0–22.0 % h^{-1}) in etiolated hypocotyls during the phase of their rapid elongation (fig. 1B in Refrégier *et al.*, 2004). Overall, the correlation analysis has revealed three factors contributing to the XTH

Table 1. *In vitro* cell wall extensibility (φ) and *in vitro* yield threshold (*y*) of *Arabidopsis* hypocotyl cell walls

	Four-day-old hypocotyls				Seven-day-old hypocotyls			
Line	pH 6.0		pH 5.0		pH 6.0		pH 5.0	
	φ[a]	*y*[b]	φ	*y*	φ	*y*	φ	*y*
Wild type	0.11±0.05	22.3±11.7	0.55±0.30	20.1±10.4	0.11±0.02	21.5±3.4	0.44±0.28	19.0±9.7
AtXTH18	0.12±0.06	12.6±8.2	0.57±0.19	14.8±2.7	0.11±0.04	15.5±7.4	0.64±0.13	18.5±2.8
AtXTH19	0.12±0.04	8.4±5.6	0.92±0.08	14.0±0.7	0.12±0.03	19.3±3.2	0.53±0.15	18.8±4.5
AtXTH20	0.11±0.07	11.7±6.5	0.67±0.28	14.3±3.4	0.21±0.04	16.6±2.4	0.68±0.08	15.4±1.3
PttXET	0.15±0.08	13.1±4.6	1.02±0.64	15.8±4.5	0.18±0.04	19.8±2.4	0.49±0.20	17.6±5.0

[a] φ values (± SE) corresponding to slopes of the fitted straight lines in Fig. 5 are expressed in % h^{-1} MPa^{-1}.
[b] *y* values (± SE) corresponding to intercepts of the fitted straight lines with the abscissa in Fig. 5 are expressed in MPa.

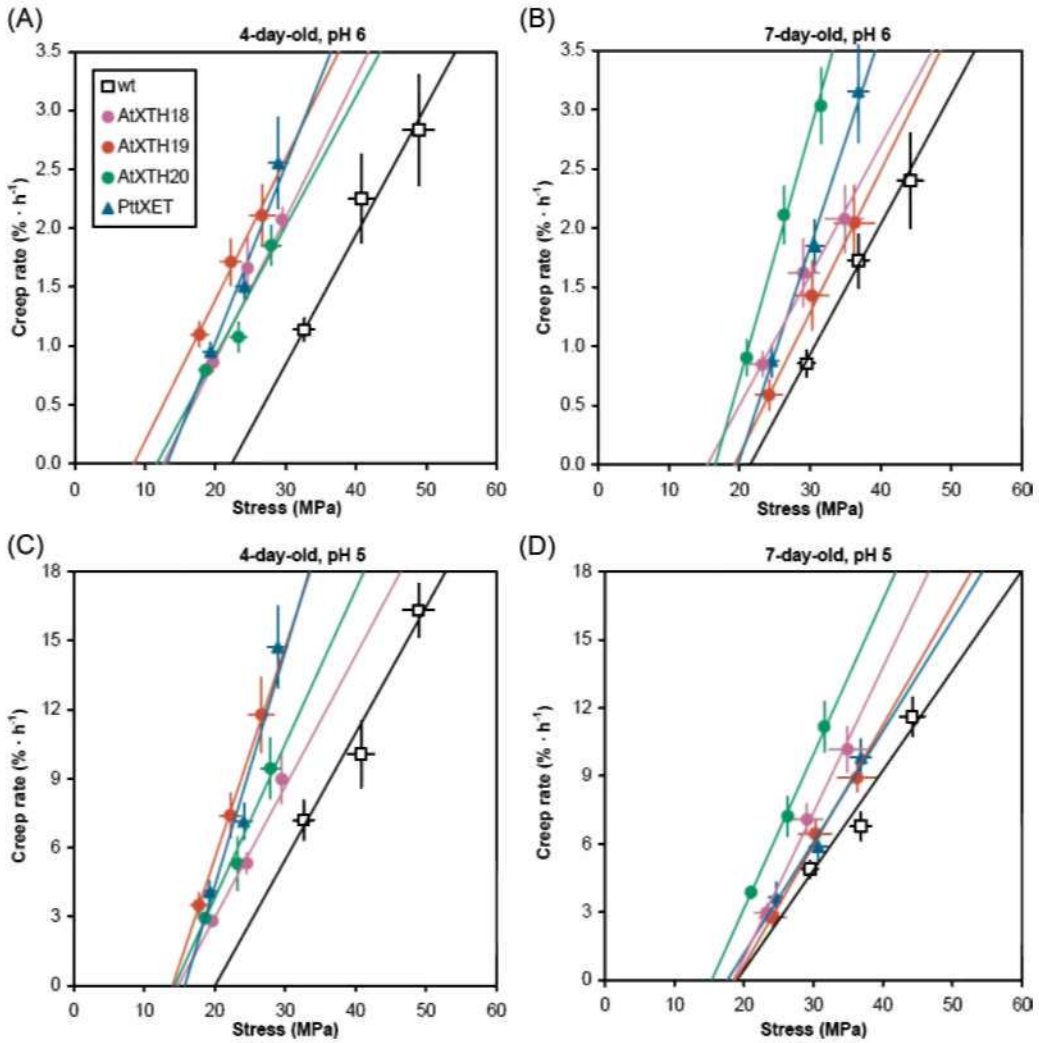

Fig. 5. Dependence of creep rate of frozen/thawed *Arabidopsis* hypocotyls on the applied uniaxial stress. The data refer to (A) hypocotyls of 4-day-old plants extended at pH 6.0; (B) hypocotyls of 7-day-old plants extended at pH 6.0; (C) hypocotyls of 4-day-old plants extended at pH 5.0; (D) hypocotyls of 7-day-old plants extended at pH 5.0. Creep rate and stress values were taken from Supplementary Fig. S7 and Supplementary Table S5 at *JXB* online, respectively, and are reported with their standard errors. The straight lines were fitted to the data using the Deming regression taking into account the error in both creep rate (Supplementary Fig. S7) and wall stress (Supplementary Table S5). Note that the ordinate axes are scaled differently for the pH 6.0 (A, B) and the pH 5.0 (C, D) data.

overexpression-induced growth stimulation in *Arabidopsis* hypocotyls: increased normalized initial deformations, lower y values, and higher ability for long-term extension expressed in the form of the more linear creep.

Discussion

XTH overexpression, XET activity, and growth of Arabidopsis *hypocotyls*

It was described in the present study that overexpression of different *XTH* genes had diverse effects on growth of etiolated *Arabidopsis* hypocotyls (Fig. 1). Their expansion in the three lines overexpressing *Arabidopsis XTH* genes was stimulated to a different extent. On the other hand, heterologous ectopic expression of the aspen *XTH* gene did not affect growth of *Arabidopsis* hypocotyls. These results are in line with the reports on *XTH* overexpression in plants that either stimulated growth (Shin *et al.*, 2006; Liu *et al.*, 2007; Nishikubo *et al.*, 2011) or had no effect (Genovesi *et al.*, 2008; Miedes *et al.*, 2011). The ability to modulate growth may thus be specific for particular XTHs, which is well illustrated by *AtXTH18*. This *XTH* had the lowest level of overexpression (2-fold) in the expanding hypocotyls among all the *XTH* genes studied but produced the highest growth stimulation (Fig. 1A). Interestingly, as little as only 14% reduction in the level of AtXTH18 mRNA by RNA interference (RNAi) technology led to significant growth inhibition in *Arabidopsis* roots (Osato *et al.*, 2006). Apparently AtXTH18 does play an important role during growth in *Arabidopsis*. Despite the fact that AtXTH18, AtXTH19, and AtXTH20 are considered as root-specific enzymes (Yokoyama and Nishitani, 2001; Vissenberg *et al.*, 2005), their expression was also detected in wild-type *Arabidopsis* hypocotyls (Becnel *et al.*, 2006; Jamet *et al.*, 2009). Unlike other *AtXTH* genes studied here, *AtXTH19* demonstrated a high level of expression in etiolated wild-type hypocotyls comparable with that of the shoot-specific *AtXTH4*, *AtXTH8*, *AtXTH15*, *AtXTH24*, *AtXTH27*, and *AtXTH30* (Jamet *et al.*, 2009). This could explain the complex effect of *AtXTH19* overexpression involving the initial growth inhibition (and/or delay in germination) followed by its stimulation (Fig. 1B; Supplementary Table S2 at *JXB* online). The activity of AtXTH19 increased by overexpression could simply become saturating or even superoptimal for growth during some stages of hypocotyl development. PttXET16-34 stimulated radial expansion of vessel elements in aspen (Nishikubo *et al.*, 2011) but had no significant effect on growth in *Arabidopsis* hypocotyls (Fig. 1). This absence of the growth effect may be explained by different pH optima and substrate specificities between the aspen XTH and the AtXTHs studied (Saura-Valls *et al.*, 2006; Maris *et al.*, 2011), such that conditions in the cell walls of *Arabidopsis* could be non-optimal for PttXET16-34. Another explanation may be the fact that *PttXET16-34* overexpression increased the level of phenolics and decreased the level of acidic pectins in the cell walls via an unknown mechanism (Supplementary Fig. S3, Supplementary Table S3). The resulting changes in the wall hydrophobicity and pH could establish less favourable conditions for different cell wall-loosening proteins, thus eliminating the potential growth stimulation that may have been caused by the increased XET activity in the PttXET16-34 line (Fig. 2A). Nevertheless, the majority of the XTH-OE lines did not demonstrate any significant increase in total XET activity over the wild type in growing 4-day-old hypocotyls (Fig. 2A), which may result from a masking effect of XET activity by the endogenous XTH enzymes (Genovesi *et al.*, 2008). The reported increase in XET activity in non-expanding 7-day-old hypocotyls (Fig. 2A) could reflect the involvement of some XTHs in vascular differentiation rather than in growth regulation, as was shown in different *Arabidopsis* organs (Matsui *et al.*, 2005; Vissenberg *et al.*, 2005; Yokoyama and Nishitani, 2006).

Optimization of conditions for measuring cell wall properties relevant for growth

In the present work, the creep test was used under conditions optimized for measurements of wall physical properties relevant for growth of etiolated *Arabidopsis* hypocotyls. The 5 mm long subapical hypocotyl segments used in extensiometry (Supplementary Fig. S1 at *JXB* online) allowed comparison of the wall properties of growing versus non-growing hypocotyls. These segments include a significant part of the growth zone in 4-day-old hypocotyls and contain few if any expanding cells in 7-day-old hypocotyls (Gendreau *et al.*, 1997). To the authors' knowledge, the pH values in the apoplast of *Arabidopsis* hypocotyls have never been reported. Accordingly, the choice of pH 6.0 and pH 5.0 buffers for extensiometry was based on the physiological pH range measured in the plant apoplast (Monshausen *et al.*, 2009). It was also taken into account that cell wall acidification to or below pH 5.0 is usually involved in the mechanism of growth stimulation in different plant organs (Rayle and Cleland, 1992; Bibikova *et al.*, 1998; Fasano *et al.*, 2001). The *in vitro* stress of 17.8–48.9 MPa generated in the cell walls of frozen/thawed hypocotyls (Supplementary Table S5) is comparable with that caused by turgor *in vivo* in growing cell walls (~10–50 MPa) (Szymanski and Cosgrove, 2009). *In vitro* extension of hypocotyls at the physiologically relevant pH and stress values was characterized by creep rates very similar to the growth rates of cells in dark-grown *Arabidopsis* hypocotyls (compare Supplementary Fig. S7A, C with fig. 1B in Refrégier *et al.*, 2004), confirming the adequacy of conditions used for extensiometry.

In vitro *acid-induced extension in* Arabidopsis *hypocotyls and its possible mechanism*

The strong stimulatory effect of the pH 5.0 buffer on creep had a non-specific character as it was observed in all hypocotyls studied (Supplementary Tables S6–S8, Supplementary Fig. S7, S8 at *JXB* online). This effect was protein dependent as it completely disappeared after a heat treatment that inactivated cell wall proteins (E. Miedes *et al.*, unpublished results). Two protein classes have been known for their role in the stimulation of acid-induced cell wall extension: expansins

(McQueen-Mason *et al.*, 1992) and yieldins (Okamoto-Nakazato *et al.*, 2000). Expansins were reported simultaneously to increase φ (*in vitro* cell wall extensibility) and decrease y (*in vitro* cell wall yield threshold) in isolated cell walls (Takahashi *et al.*, 2006), while yieldins exerted their effect exclusively by decreasing y (Okamoto-Nakazato *et al.*, 2000). In the present study, the pH 5.0 buffer had a weak if any influence on y but greatly increased φ (Fig. 5, Table 1). This effect must have been primarily caused by expansins which, unlike yieldins, are abundantly expressed in etiolated *Arabidopsis* hypocotyls (Irshad *et al.*, 2008; Jamet *et al.*, 2009).

The contribution of XTHs to the acid-induced wall extension *in vitro* could hardly be significant as they are usually more active at neutral than at acidic pH. In particular, this was demonstrated for AtXTH4 and AtXTH24, the most highly expressed XTHs in wild-type *Arabidopsis* hypocotyls (Campbell and Braam, 1999; Irshad *et al.*, 2008; Jamet *et al.*, 2009), and for AtXTH18 and AtXTH19 whose activities were much lower at pH 5.0 versus pH 6.0 (Maris *et al.*, 2011). However, PttXET16-34 is more active at pH 5.0 than at pH 6.0 (Saura-Valls *et al.*, 2006). Nevertheless, despite the higher total XET activity in hypocotyls of the PttXET-OE line (Fig. 2A), the acidic buffer did not make them relatively more extensible compared with hypocotyls of other XTH-OE lines (Supplementary Fig. S7A, C). Apparently PttXET16-34 does not contribute to the acid-induced extension.

In contrast to creep rate, initial deformation was unaffected or decreased at pH 5.0 (Fig. 3; Supplementary Tables S6–S8 at *JXB* online), emphasizing their different nature. Creep was shown to be mostly irreversible (plastic) wall extension, while initial deformation comprised a significant reversible (elastic or viscoelastic) component (Nolte and Schopfer, 1997; Suslov and Verbelen, 2006). Cell walls were reported to swell under acidic conditions (Thompson, 2005). Such swelling at pH 5.0 may facilitate irreversible slippage of wall polymers past each other while interfering with their reversible reorientation in the direction of strain. The reorientation causes shear and compression between wall polymers (Burgert and Fratzl, 2007) that will be increasing due to accumulation of incompressible water upon the wall swelling. Thus, the acid-induced changes in initial deformation may result from a balance between the opposite effects of the pH 5.0 buffer on plastic and elastic wall extension.

Age-dependent changes in cell wall properties of Arabidopsis *hypocotyls*

Age-dependent changes in cell wall properties associated with growth cessation in hypocotyls included a decrease in initial deformation, an increase in y, and changes in the linearity of creep. The decrease in initial deformation in 7-day-old versus 4-day-old hypocotyls was not affected by acidic pH or *XTH* overexpression (Fig. 3; Supplementary Tables S6–S8 at *JXB* online). It could result from changes in growth-relevant cell wall properties that are not directly controlled by expansins or XTHs. This effect might be mediated by cellulose microfibrils attaining a more axial orientation in *Arabidopsis* hypocotyls during their growth (Refrégier *et al.*, 2004). Cellulose realignment in the direction of strain is known to cause strain hardening of the wall, making it progressively stiffer in the direction of microfibril reorientation (Matas *et al.*, 2004; Burgert and Fratzl, 2007; Suslov *et al.*, 2009). Initial deformation was indeed lower in the direction of the net cellulose alignment in *Nitella* and onion cell walls (Richmond *et al.*, 1980; Suslov and Verbelen, 2006). The age-dependent increase in y (Table 1) can also result from the axial cellulose realignment during elongation of *Arabidopsis* hypocotyls. In *Nitella* cell walls, y was higher parallel to the preferential microfibril orientation than transverse to it (Métraux and Taiz, 1978). Additionally, the age-dependent changes in initial deformation and y may result from a tyrosine-based cross-linking of cell wall structural proteins (Ding and Zhu, 1997; De Cnodder *et al.*, 2005). Another mechanism of these changes consistent with the data of FT-IR analysis (Supplementary Fig. S4; Supplementary Table S4) may involve a reduction of pectin esterification. Less esterified pectins are more prone to calcium-mediated cross-linking, which may strengthen cell walls (Jarvis, 1984). These processes were observed in plant axial organs during growth cessation (Lieberman *et al.*, 1999), in the course of wood cell expansion (Siedlecka *et al.*, 2008), and could also work in *Arabidopsis* hypocotyls (Derbyshire *et al.*, 2007*b*; Abasolo *et al.*, 2009).

Growth cessation of hypocotyls was associated with a significant drop in linearity of creep at pH 5.0 (Fig. 4; Supplementary Table S9 at *JXB* online). This effect could be mediated by different interactions between cell wall matrix and cellulose microfibrils during extension of 4- and 7-day-old hypocotyls. In the younger hypocotyls, cellulose microfibrils are oriented transversally to the axis of elongation (Refrégier *et al.*, 2004). In this case considerable cell wall extension could proceed via separation of parallel microfibrils without their significant reorientation (Marga *et al.*, 2005). Such extension seems to be accompanied by high tensile stress in the wall matrix with little or no shear and compressive stresses (Burgert and Fratzl, 2007). Accordingly, it is the resistance of the wall matrix to tensile stress that could limit extension of 4-day-old hypocotyls. This resistance can be decreased by expansins at the acidic pH allowing the practically linear cell wall extension in 4-day-old hypocotyls at pH 5.0 (Fig. 4C). On the other hand, cellulose microfibrils are tilted towards the axis in more mature hypocotyls (Refrégier *et al.*, 2004). In this case, cell wall extension involves further realignment of microfibrils in the direction of strain, which is accompanied not only by tensile stress but also by significant shear and compression in the matrix (Burgert and Fratzl, 2007). This shear and compression will be progressively increasing during *in vitro* extension of 7-day-old hypocotyls, leading to a decay in the creep rate over time (Fig. 4D). Thus, the age-dependent decrease in linearity of creep at pH 5.0 (Fig. 4C, D) may result from higher shear and compression developing in the wall matrix of 7-day-old hypocotyls that interfere with axial cellulose reorientation.

Changes in cell wall properties of Arabidopsis *hypocotyls related to XTH overexpression*

XTH overexpression stimulated deposition of polymeric material in *Arabidopsis* hypocotyl cell walls (Supplementary

Table S5 at *JXB* online), which was more pliant than in wild-type walls because of higher initial deformation·stress^{-1} and lower y values (Figs 3, 5, Table 1). Additionally, creep of growing hypocotyls was usually more linear in XTH-OE lines than in the wild type (Fig. 4C, Supplementary Table S9).

Although XET activity can incorporate newly secreted xyloglucans into the existing wall matrix (Antosiewicz *et al.*, 1997; Mellerowicz *et al.*, 2008; Maris *et al.*, 2009; Nishikubo *et al.*, 2011), this process alone could hardly explain a >65% increase in the wall weight in XTH-OE lines (Supplementary Table S5 at *JXB* online). If it were a direct consequence of xyloglucan incorporation by XET activity increasing its proportion in the wall, the respective changes in the FT-IR spectra would be seen. This, however, was not observed (Supplementary Fig. S3, Supplementary Table S3), implying mostly an indirect effect of *XTH* overexpression on accumulation of the the wall material. Cell wall synthesis and thickening in young (up to 2-day-old) slowly growing *Arabidopsis* hypocotyls are required for their subsequent growth acceleration (Refrégier *et al.*, 2004; Derbyshire *et al.*, 2007*a*; Pelletier *et al.*, 2010). This phase of rapid growth is suppressed by both blocking cellulose synthesis (Refrégier *et al.*, 2004) and disturbing its correct transverse orientation (MacKinnon *et al.*, 2006) during early development of hypocotyls. *XTH* overexpression decreased y and increased initial deformation·stress^{-1} and the linearity of creep in 4-day-old hypocotyls (Table 1, Fig. 3A, C, Supplementary Table S9), the characteristics being dependent on cellulose microfibrils, as discussed above. Therefore, it is hypothesized that *XTH* overexpression may indirectly modify the *Arabidopsis* walls by affecting cellulose synthesis and deposition. The overexpression and the resulting XET activity in young (up to 2-day-old) hypocotyls could create a loosened wall matrix adjacent to cellulose synthase complexes exerting lower resistance to their movement in the plasmalemma. This could accelerate cellulose deposition and decrease the deviation of microfibril alignment from the direction defined by cortical microtubules (Paredez *et al.*, 2006; Crowell *et al.*, 2011). Additionally, the overexpression-induced changes in the wall matrix in the vicinity of nascent microfibrils may affect the cellulose crystallinity, another factor involved in the growth regulation of *Arabidopsis* hypocotyls (Fujita *et al.*, 2011). Unfortunately, 2-day-old hypocotyls active in cellulose synthesis are too short to be directly analysed in the creep test.

The wall material accumulation was observed in all the XTH-OE lines (Supplementary Table S5 at *JXB* online). However, in the PttXET16-34-OE line, it was not accompanied by growth stimulation (Fig. 1). Hence, this quantitative change in cell walls could be necessary but insufficient for the growth effect in hypocotyls. Additional *XTH* overexpression-mediated growth-stimulatory mechanisms may involve a higher rate of cutting and rejoining of xyloglucan chains between cellulose microfibrils by XET activity. This process will only change the mass distributions of xyloglucans in cell walls (Peña *et al.*, 2004; Nishikubo *et al.*, 2011), which cannot be detected by the FT-IR analysis used here. The XET activity of PttXET16-34 with *Arabidopsis* xyloglucans may be lower than that of the rest of the XTHs studied, explaining why the former did not stimulate hypocotyl growth.

The present results show that XTHs change the wall mechanics by a different mechanism compared with expansins. As seen from the influence of the pH 5.0 buffer, expansins act by increasing φ, while XTHs decrease y of *Arabidopsis* cell walls (Fig. 5A, C; Table 1). This XTH effect cannot be mediated by expansins, as it is present at pH 6.0 when expansins are inactive (McQueen-Mason *et al.*, 1992; Takahashi *et al.*, 2006).

Thus, the present study suggests that only particular XTH enzymes are involved in the growth regulation. Their mechanism of action may combine a rather indirect effect on the wall synthesis with a direct XET-mediated molecular grafting of xyloglucans. A detailed compositional and architectural wall analysis is needed to explain the XTH-induced changes in the cell wall physical properties.

Supplementary data

Supplementary data are available at *JXB* online.

Figure S1. Positions of hypocotyl segments analysed in *Arabidopsis* seedlings.

Figure S2. Time-dependent extension (creep) of frozen/thawed *Arabidopsis* hypocotyls in a uniaxial constant-load test.

Figure S3. FT-IR analysis of differences in cell wall composition between the wild type and XTH-overexpressing lines.

Figure S4. FT-IR analysis of age-dependent changes in cell wall composition of the wild type and XTH-overexpressing lines.

Figure S5. Principal component analysis of FT-IR spectra of cell wall material from 4- and 7-day-old hypocotyls of the wild type and XTH-overexpressing lines.

Figure S6. Dependence of initial deformation of frozen/thawed *Arabidopsis* hypocotyls on the applied uniaxial stress.

Figure S7. Creep rate of frozen/thawed *Arabidopsis* hypocotyls *in vitro*.

Figure S8. Normalized creep rate (creep rate·stress^{-1}) of frozen/thawed *Arabidopsis* hypocotyls *in vitro*.

Table S1. Oligonucleotides used in this study.

Table S2. Length of hypocotyls in 2- to 7-day-old etiolated *Arabidopsis* plants.

Table S3. Significant differences in cell wall composition of 4- and 7-day-old hypocotyls of XTH-OE lines compared with the wild type.

Table S4. Significant age-dependent differences in cell wall composition of *Arabidopsis* hypocotyls from wild type and XTH-OE plants.

Table S5. Tensile stresses generated in hypocotyls *in vitro* under a constant load.

Table S6. Extension of *Arabidopsis* hypocotyls induced by a 500 mg load.

Table S7. Extension of *Arabidopsis* hypocotyls induced by a 625 mg load.

Table S8. Extension of *Arabidopsis* hypocotyls induced by a 750 mg load.

Table S9. Linearity of time-dependent extension of *Arabidopsis* hypocotyls.

Table S10. Correlation analysis of growth rate and cell wall biomechanical characteristics.

Acknowledgements

This work was supported by grants from the Research Foundation–Flanders (FWO) [grant nos WO038.04 N and G.0524.07], the University of Antwerp (BOF-NOI) and Ghent University, the Interuniversity Attraction Poles Programme–Belgian State–Belgian Science Policy [IUAP VI/33]. FV is a post-doctoral fellow of the Research Foundation–Flanders (FWO). The authors acknowledge Dr Band (Centre for Plant Integrative Biology, University of Nottingham) for her help with regression analysis, Professor Cool (Department of Chemistry, University of Antwerp) for the use of the high-precision balance Mettler M3, Professor Blust (Department of Biology, University of Antwerp) for the use of the iCycler (Roche) Real Time qRT–PCR setup, and Professor Herrebout (Department of Chemistry, University of Antwerp) for the use of the FT-IR setup.

References

Abasolo W, Eder M, Yamauchi K, *et al.* 2009. Pectin may hinder the unfolding of xyloglucan chains during cell deformation: implications of the mechanical performance of *Arabidopsis* hypocotyls with pectin alterations. *Molecular Plant* **2,** 990–999.

Antosiewicz DM, Purugganan MM, Polisensky DH, Braam J. 1997. Cellular localization of Arabidopsis xyloglucan endotransglycosylase-related proteins during development and after wind stimulation. *Plant Physiology* **115,** 1319–1328.

Baumann MJ, Eklöf JM, Michel G, Kallas ÅM, Teeri TT, Czjzek M, Brumer H. 2007. Structural evidence for the evolution of xyloglucanase activity from xyloglucan endo-transglycosylases: biological implications for cell wall metabolism. *The Plant Cell* **19,** 1947–1963.

Becnel J, Natarajan M, Kipp A, Braam J. 2006. Developmental expression patterns of Arabidopsis XTH genes reported by transgenes and Genevestigator. *Plant Molecular Biology* **61,** 451–467.

Benjamini Y, Hochberg Y. 1995. Controlling the false discovery rate: a practical and powerful approach to multiple testing. *Journal of the Royal Statistical Society. Series B (Methodological)* **57,** 289–300.

Bibikova TN, Jacob T, Dahse I, Gilroy S. 1998. Localized changes in apoplastic and cytoplasmic pH are associated with root hair development in *Arabidopsis thaliana*. *Development* **125,** 2925–2934.

Bichet A, Desnos T, Turner S, Grandjean O, Höfte H. 2001. *BOTERO1* is required for normal orientation of cortical microtubules and anisotropic cell expansion in *Arabidopsis*. *The Plant Journal* **25,** 137–148.

Bradford MM. 1976. A rapid and sensitive method for quantification of microgram quantities of protein utilizing the principle of protein–dye binding. *Analytical Biochemistry* **72,** 248–252.

Burgert I, Fratzl P. 2007. Mechanics of the expanding cell wall. In: Verbelen J-P, Vissenberg K, eds. *The expanding cell. Plant Cell Monographs Vol. 5* . Berlin: Springer, 191–215.

Campbell P, Braam J. 1999. *In vitro* activities of four xyloglucan endotransglycosylases from *Arabidopsis*. *The Plant Journal* **18,** 371–382.

Carpita NC, Gibeaut DM. 1993. Structural models of primary cell walls in flowering plants: consistency of molecular structure with the physical properties of the walls during growth. *The Plant Journal* **3,** 1–30.

Cavalier DM, Lerouxel O, Neumetzler L, *et al.* 2008. Disrupting two *Arabidopsis thaliana* xylosyltransferase genes results in plants deficient in xyloglucan, a major primary cell wall component. *The Plant Cell* **20,** 1519–1537.

Cleland R. 1967. Extensibility of isolated cell walls: measurement and changes during cell elongation. *Planta* **74,** 197–209.

Clough SJ, Bent AF. 1998. Floral dip: a simplified method for Agrobacterium-mediated transformation of Arabidopsis thaliana. *The Plant Journal* **16,** 735–743.

Cosgrove DJ. 1989. Characterization of long-term extension of isolated cell walls from growing cucumber hypocotyls. *Planta* **177,** 121–130.

Cosgrove DJ. 1993. Wall extensibility: its nature, measurement and relationship to plant cell growth. *New Phytologist* **124,** 1–23.

Cosgrove DJ. 2000. Loosening of plant cell walls by expansins. *Nature* **407,** 321–326.

Crowell EF, Timpano H, Desprez T, Franssen-Verheijen T, Emons AM, Höfte H, Vernhettes S. 2011. Differential regulation of cellulose orientation at the inner and outer face of epidermal cells in the Arabidopsis hypocotyl. *The Plant Cell* **23,** 2592–2605.

De Cnodder T, Vissenberg K, Van Der Straeten D, Verbelen J-P. 2005. Regulation of cell length in the *Arabidopsis thaliana* root by the ethylene precursor 1-aminocyclopropane-1-carboxylic acid: a matter of apoplastic reactions. *New Phytologist* **168,** 541–550.

Derbyshire P, Findlay K, McCann MC, Roberts K. 2007*a*. Cell elongation in *Arabidopsis* hypocotyls involves dynamic changes in cell wall thickness. *Journal of Experimental Botany* **58,** 2079–2089.

Derbyshire P, McCann MC, Roberts K. 2007*b*. Restricted cell elongation in Arabidopsis hypocotyls is associated with a reduced average pectin esterification level. *BMC Plant Biology* **7,** 31.

Ding L, Zhu J-K. 1997. A role for arabinogalactan-proteins in root epidermal cell expansion. *Planta* **203,** 289–294.

Estelle MA, Somerville C. 1987. Auxin-resistant mutants of Arabidopsis thaliana with an altered morphology. *Molecular and General Genetics* **206,** 200–206.

Fasano JM, Swanson SJ, Blancaflor EB, Dowd PE, Kao TH, Gilroy S. 2001. Changes in root cap pH are required for the gravity response of the Arabidopsis root. *The Plant Cell* **13,** 907–921.

Fry SC, Smith RC, Renwick KF, Martin DJ, Hodge SK, Matthews KJ. 1992. Xyloglucan endotransglycosylase, a new wall-loosening enzyme activity from plants. *Biochemical Journal* **282,** 821–828.

Fujita M, Himmelspach R, Hocart CH, Williamson RE, Mansfield SD, Wasteneys GO. 2011. Cortical microtubules optimize cell-wall crystallinity to drive unidirectional growth in Arabidopsis. *The Plant Journal* **66,** 915–928.

Gendreau E, Traas J, Desnos T, Grandjean O, Caboche M, Höfte H. 1997. Cellular basis of hypocotyl growth in Arabidopsis thaliana. *Plant Physiology* **114,** 295–305.

Genovesi V, Fornalé S, Fry SC, *et al.* 2008. ZmXTH1, a new xyloglucan endotransglucosylase/hydrolase in maize, affects cell wall structure and composition in *Arabidopsis thaliana*. *Journal of Experimental Botany* **59,** 875–889.

Gibson LJ. 2012. The hierarchical structure and mechanics of plant materials. *Journal of the Royal Society Interface* **9,** 2749–2766.

Green PB. 1976. Growth and cell pattern formation on an axis: critique of concepts, terminology, and models of study. *Botanical Gazette* **137,** 187–202.

Handford MG, Baldwin TC, Goubet F, Prime TA, Miles J, Yu X, Dupree P. 2003. Localisation and characterisation of cell wall mannan polysaccharides in *Arabidopsis thaliana*. *Planta* **218,** 27–36.

Ibatullin FI, Banasiak A, Baumann MJ, Greffe L, Takahashi J, Mellerowicz EJ, Brumer H. 2009. A real-time fluorogenic assay for the visualization of glycoside hydrolase activity in planta. *Plant Physiology* **151,** 1741–1750.

Irshad M, Canut H, Borderies G, Pont-Lezica R, Jamet E. 2008. A new picture of cell wall protein dynamics in elongating cells of *Arabidopsis thaliana*: confirmed actors and newcomers. *BMC Plant Biology* **8,** 94.

Jamet E, Roujol D, San-Clemente H, Irshad M, Soubigou-Taconnat L, Renou JP, Pont-Lezica R. 2009. Cell wall biogenesis of *Arabidopsis thaliana* elongating cells: transcriptomics complements proteomics. *BMC Genomics* **10,** 505.

Jarvis MC. 1984. Structure and properties of pectin gels in plant cell walls. *Plant, Cell and Environment* **7,** 153–164.

Kallas ÅM, Piens K, Denman S, Henriksson H, Fäldt J, Johansson P, Brumer H, Teeri TT. 2005. Enzymatic properties of native and deglycosylated hybrid aspen (*Populus tremula tremuloides*) xyloglucan endotransglycosylase 16A expressed in *Pichia pastoris*. *Biochemical Journal* **390,** 105–113.

Karimi M, Inze D, Depicker A. 2002. Gateway vectors for Agrobacterium-mediated plant transformation. *Trends in Plant Science* **7,** 193–195.

Köhler L, Spatz H-C. 2002. Micromechanics of plant tissues beyond the linear-elastic range. *Planta* **215,** 33–40.

Liberman M, Mutaftschiev S, Jauneau A, Vian B, Catesson AM, Goldberg R. 1999. Mung bean hypocotyl homogalacturonan: localization, organization and origin. *Annals of Botany* **84,** 225–233.

Liu YB, Lu SM, Zhang JF, Liu S, Lu YT. 2007. A xyloglucan endotransglucosylase/hydrolase involves in growth of primary roots and alters the deposition of cellulose in Arabidopsis. *Planta* **226,** 1547–1560.

Lorences EP, Fry SC. 1993. Xyloglucan oligosaccharides with at least two α-D-xylose residues acts as an acceptor for xyloglucan endotransglycosylase and promote the depolymerization of xyloglucan. *Physiologia Plantarum* **88,** 105–112.

MacKinnon IM, Sturcová A, Sugimoto-Shirasu K, His I, McCann MC, Jarvis MC. 2006. Cell-wall structure and anisotropy in procuste, a cellulose synthase mutant of *Arabidopsis thaliana*. *Planta* **224,** 438–448.

MacMillan CP, Mansfield SD, Stachurski ZH, Evans R, Southerton SG. 2010. Fasciclin-like arabinogalactan proteins: specialization for stem biomechanics and cell wall architecture in Arabidopsis and *Eucalyptus*. *The Plant Journal* **62,** 689–703.

Marga F, Grandbois M, Cosgrove DJ, Baskin TI. 2005. Cell wall extension results in the coordinate separation of parallel microfibrils: evidence from scanning electron microscopy and atomic force microscopy. *The Plant Journal* **43,** 181–190.

Maris A, Suslov D, Fry SC, Verbelen J-P, Vissenberg K. 2009. Enzymic characterization of two recombinant xyloglucan endotransglucosylase/hydrolase (XTH) proteins of *Arabidopsis* and their effect on root growth and cell wall extension. *Journal of Experimental Botany* **60,** 3959–3972.

Maris A, Kaewthai N, Eklöf JM, Miller JG, Brumer H, Fry SC, Verbelen J-P, Vissenberg K. 2011. Differences in enzymic properties of five recombinant xyloglucan endotransglucosylase/hydrolase (XTH) proteins of *Arabidopsis thaliana*. *Journal of Experimental Botany* **62,** 261–271.

Matas AJ, Cobb ED, Bartsch JA, Paolillo DJ Jr, Niklas KJ. 2004. Biomechanics and anatomy of *Lycopersicon esculentum* fruit peels and enzyme-treated samples. *American Journal of Botany* **91,** 352–360.

Matsui A, Yokoyama R, Seki M, Ito T, Shinozaki K, Takahashi T, Komeda Y, Nishitani K. 2005. AtXTH27 plays an essential role in cell wall modification during the development of tracheary elements. *The Plant Journal* **42,** 525–534.

McQueen-Mason S, Durachko DM, Cosgrove DJ. 1992. Two endogenous proteins that induce cell wall extension in plants. *The Plant Cell* **4,** 1425–1433.

Mellerowicz EJ, Immerzeel P, Hayashi T. 2008. Xyloglucan: the molecular muscle of trees. *Annals of Botany* **102,** 659–665.

Métraux J-P, Taiz L. 1978. Transverse viscoelastic extension in *Nitella*: I. Relationship to growth rate. *Plant Physiology* **61,** 135–138.

Miedes E, Lorences PE. 2004. Apple (*Malus domestica*) and tomato (*Lycopersicum esculentum*) fruits cell-wall hemicelluloses and xyloglucan degradation during *Penicillium expansum* infection. *Journal of Agricultural and Food Chemistry* **52,** 7957–7963.

Miedes E, Lorences EP. 2009. Xyloglucan endotransglucosylase/hydrolases (XTHs) during tomato fruit growth and ripening. *Journal of Plant Physiology* **166,** 489–498.

Miedes E, Zarra I, Hoson T, Herbers K, Sonnewald U, Lorences EP. 2011. Xyloglucan endotransglucosylase and cell wall extensibility. *Journal of Plant Physiology* **168,** 196–203.

Monshausen GB, Bibikova TN, Weisenseel MH, Gilroy S. 2009. Ca^{2+} regulates reactive oxygen species production and pH during mechanosensing in Arabidopsis roots. *The Plant Cell* **21,** 2341–2356.

Nelson N. 1944. A photometric adaptation of the Somogyi method for the determination of glucose. *Journal of Biological Chemistry* **153,** 375–381.

Nishikubo N, Takahashi J, Roos AA, Derba-Maceluch M, Piens K, Brumer H, Teeri TT, Stålbrand H, Mellerowicz EJ. 2011. Xyloglucan endo-transglycosylase-mediated xyloglucan rearrangements in developing wood of hybrid aspen. *Plant Physiology* **155,** 399–413.

Nishitani K, Vissenberg K. 2007. Roles of the XTH protein family in the expanding cell. In: Verbelen J-P, Vissenberg K, eds. *The expanding cell. Plant Cell Monographs Vol. 5* . Berlin: Springer, 89–116.

Nolte T, Schopfer P. 1997. Viscoelastic versus plastic cell wall extensibility in growing seedling organs: a contribution to avoid some misconceptions. *Journal of Experimental Botany* **48,** 2103–2107.

Okamoto H, Okamoto A. 1994. The pH-dependent yield threshold of the cell wall in a glycerinated hollow cylinder (*in vitro* system) of cowpea hypocotyl. *Plant, Cell and Environment* **17,** 979–983.

Okamoto-Nakazato A, Nakamura T, Okamoto A. 2000. The isolation of wall-bound proteins regulating yield threshold in glycerinated hollow cylinders of cowpea hypocotyls. *Plant, Cell and Environment* **23,** 145–154.

Osato Y, Yokoyama R, Nishitani K. 2006. A principal role for AtXTH18 in Arabidopsis thaliana root growth—a functional analysis using RNAi plants. *Journal of Plant Research* **119,** 153–162.

Paredez AR, Somerville CR, Ehrhardt DW. 2006. Visualization of cellulose synthase demonstrates functional association with microtubules. *Science* **312,** 1491–1495.

Park YB, Cosgrove DJ. 2012*a*. Changes in cell wall biomechanical properties in the xyloglucan-deficient xxt1/xxt2 mutant of Arabidopsis. *Plant Physiology* **158,** 465–475.

Park YB, Cosgrove DJ. 2012*b*. A revised architecture of primary cell walls based on biomechanical changes induced by substrate-specific endoglucanases. *Plant Physiology* **158,** 1933–1943.

Pelletier S, Van Orden J, Wolf S, *et al.* 2010. A role for pectin de-methylesterification in a developmentally regulated growth acceleration in dark-grown Arabidopsis hypocotyls. *New Phytologist* **188,** 726–739.

Peña MJ, Ryden P, Madson M, Smith AC, Carpita NC. 2004. The galactose residues of xyloglucan are essential to maintain mechanical strength of the primary cell walls in Arabidopsis during growth. *Plant Physiology* **134,** 443–451.

Pfaffl MW. 2001. A new mathematical model for relative quantification in real-time RT-PCR. *Nucleic Acids Research* **29,** 2002–2007.

Rayle DL, Cleland RE. 1992. The acid growth theory of auxin-induced cell elongation is alive and well. *Plant Physiology* **99,** 1271–1274.

Refrégier G, Pelletier S, Jaillard D, Höfte H. 2004. Interaction between wall deposition and cell elongation in dark-grown hypocotyl cells in Arabidopsis. *Plant Physiology* **135,** 959–968.

Reiter W-D, Chapple CC, Somerville CR. 1993. Altered growth and cell walls in a fucose-deficient mutant of *Arabidopsis*. *Science* **261,** 1032–1035.

Richmond PA, Métraux J-P, Taiz L. 1980. Cell expansion patterns and directionality of wall mechanical properties in *Nitella*. *Plant Physiology* **65,** 211–217.

Ripley BD, Thompson M. 1987. Regression techniques for the detection of analytical bias. *Analyst* **112,** 377–383.

Rose JKC, Braam J, Fry SC, Nishitani K. 2002. The XTH family of enzymes involved in xyloglucan endotransglycosylation and endohydrolysis: current perspectives and a new unifying nomenclature. *Plant and Cell Physiology* **43,** 1421–1435.

Ryden P, Sugimoto-Shirasu K, Smith AC, Findlay K, Reiter W-D, McCann MC. 2003. Tensile properties of Arabidopsis cell walls depend on both a xyloglucan cross-linked microfibrillar network and rhamnogalacturonan II–borate complexes. *Plant Physiology* **132,** 1033–1040.

Saura-Valls M, Fauré R, Ragàs S, Piens K, Brumer H, Teeri TT, Cottaz S, Driguez H, Planas A. 2006. Kinetic analysis using low-molecular mass xyloglucan oligosaccharides defines the catalytic mechanism of a Populus xyloglucan endotransglycosylase. *Biochemical Journal* **395,** 99–106.

Shin Y-K, Yum H, Kim E-S, Cho H, Gothandam KM, Hyun J, Chung Y-Y. 2006. BcXTH1, a *Brassica campestris* homologue of Arabidopsis XTH9, is associated with cell expansion. *Planta* **224,** 32–41.

Siedlecka A, Wiklundm S, Péronne MA, Micheli F, Leśniewska J, Sethson I, Edlund U, Richard L, Sundberg B, Mellerowicz EJ. 2008. Pectin methyl esterase inhibits intrusive and symplastic cell growth in developing wood of *Populus* trees. *Plant Physiology* **146,** 554–565.

Soga K, Wakabayashi K, Kamisaka S, Hoson T. 2002. Stimulation of elongation growth and xyloglucan breakdown in *Arabidopsis* hypocotyls under microgravity conditions in space. *Planta* **215,** 1040–1046.

Somogyi M. 1952. Notes on sugar determination. *Journal of Biological Chemistry* **195,** 19–23.

Suslov D, Verbelen J-P. 2006. Cellulose orientation determines mechanical anisotropy in onion epidermis cell walls. *Journal of Experimental Botany* **57,** 2183–2192.

Suslov D, Verbelen J-P, Vissenberg K. 2009. Onion epidermis as a new model to study the control of growth anisotropy in higher plants. *Journal of Experimental Botany* **60,** 4175–4187.

Szymanski DB, Cosgrove DJ. 2009. Dynamic coordination of cytoskeletal and cell wall systems during plant cell morphogenesis. *Current Biology* **19,** R800–R811.

Taiz L. 1984. Plant cell expansion: regulation of cell wall mechanical properties. *Annual Review of Plant Physiology* **35,** 585–657.

Takahashi K, Hirata S, Kido N, Katou K. 2006. Wall-yielding properties of cell walls from elongating cucumber hypocotyls in relation to the action of expansin. *Plant and Cell Physiology* **47,** 1520–1529.

Thompson DS. 2005. How do cell walls regulate plant growth? *Journal of Experimental Botany* **56,** 2275–2285.

Thompson DS. 2008. Space and time in the plant cell wall: relationships between cell type, cell wall rheology and cell function. *Annals of Botany* **101,** 203–211.

Turner SR, Somerville CR. 1997. Collapsed xylem phenotype of Arabidopsis identifies mutants deficient in cellulose deposition in the secondary cell wall. *The Plant Cell* **9,** 689–701.

Vandenbussche F, Petrasek J, Zadnikova P, *et al.* 2010. Auxin influx carriers AUX1 and LAX3 are involved in auxin–ethylene interactions during apical hook development in Arabidopsis thaliana seedlings. *Development* **137,** 597–606.

Vandenbussche F, Suslov D, De Grauwe L, Leroux O, Vissenberg K, Van Der Straeten D. 2011. The role of brassinosteroids in shoot gravitropism. *Plant Physiology* **156,** 1331–1336.

Vanzin GF, Madson M, Carpita NC, Raikhel NV, Keegstra K, Reiter W-D. 2002. The *mur2* mutant of *Arabidopsis thaliana* lacks fucosylated xyloglucan because of a lesion in fucosyltransferase AtFUT1. *Proceedings of the National Academy of Sciences, USA* **99,** 3340–3345.

Vissenberg K, Martinez-Vilchez IM, Verbelen J-P, Miller JG, Fry SC. 2000. *In vivo* co-localization of xyloglucan endotransglycosylase activity and its donor substrate in the elongation zone of Arabidopsis roots. *The Plant Cell* **12,** 1229–1238.

Vissenberg K, Oyama M, Osato Y, Yokoyama R, Verbelen J-P, Nishitani K. 2005. Differential expression of *AtXTH17*, *AtXTH18*, *AtXTH19* and *AtXTH20* genes in *Arabidopsis* roots. Physiological roles in specification in cell wall construction. *Plant and Cell Physiology* **46,** 192–200.

Walden R, Koncz C, Schell J. 1990. The use of gene vectors in plant molecular biology. *Methods in Molecular and Cellular Biology* **1**, 175–194.

Yamamoto R. 1996. Stress relaxation property of the cell wall and auxin-induced cell elongation. *Journal of Plant Research* **109,** 75–84.

Yokoyama R, Nishitani K. 2001. A comprehensive expression analysis of all members of a gene family encoding cell-wall enzymes allowed us to predict cis-regulatory regions involved in cell-wall construction in specific organs of Arabidopsis. *Plant and Cell Physiology* **42,** 1025–1033.

Yokoyama R, Nishitani K. 2006. Identification and characterization of *Arabidopsis thaliana* genes involved in xylem secondary cell walls. *Journal of Plant Research* **119,** 189–194.